04ICES-75

Experimental and Analytical Investigation of Pressure Differentials for Clean and Loaded Wire Meshes Used in Zeolite Retention

James C. Knox
NASA Marshall Space Flight Center

ABSTRACT

Following failure of the carbon dioxide removal assembly (CDRA) on the ISS, a CDRA teardown, test, and evaluation (TT&E) effort found that the sorbent material was not retained as intended by the packed beds and that presence of the sorbent in the check valve and selector valve was the cause of the failure of these components. This paper documents the development of design data for an in-line filter element. The purpose of the in-line filter is to provide temporary protection for on-orbit CDRA hardware until the bed retainment system can be redesigned and replaced.

INTRODUCTION

The design process included a review of filter media types and applicability, examination of correlations for filter media pressure drop, and use of pleated media for this application. Results of clean and loaded media pressure differential testing are presented and compared with predictions. Four prototype element geometries were tested, two procured and two fabricated by the Marshall Space Flight Center (MSFC) test team. Estimates of pressure differential for various filter medias and geometries using anchored predictive models are presented. Finally, a recommendation for an optimized filter media and geometry is made based on predictive models and pressure drop test data.

CDRA DESCRIPTION

As show in Figure 1, the CDRA is tightly integrated and mounted on slides for installation in the Atmosphere Revitalization System rack. Air selector valves are visibly numbered 101 through 106. The blower and precooler orbital replacement unit (ORU) is visible in the right center section of the drawing. Process air and coolant water interfaces are on the lower right of the drawing. The sorbent beds are not clearly visible, but are behind the valves and tubing. Controllers for the bed heaters, air-save pump, and blower are on the left side, identified by the many electrical connectors. The air-save pump resides below the controllers.

The operation of the CDRA can be explained with the aid of the schematic shown in Figure 2. The CDRA continuously removes carbon dioxide (CO_2) from the ISS atmosphere. The four beds consist of two desiccant beds and two CO_2 sorbent beds. The system operates such that one desiccant bed and one CO_2 sorbent bed are adsorbing while the other two beds are desorbing. When a new half cycle begins, the beds switch sorbent modes. The incoming air stream to the CDRA is downstream of a condensing heat exchanger, and has a dewpoint and drybulb temperature of 4.4 to 10°C (40 to 50 °F) [1]. The air stream passes first through a desiccant bed to remove virtually all of the moisture from the process air. The temperature of the air stream rises as it flows through the desiccant bed due to the heat of adsorption. The process air is then drawn through the system blower and then through an air-liquid heat exchanger or precooler. The precooler increases CO_2 sorbent efficiency by reducing process air temperature before entering the CO_2 sorbent bed. Prior to returning to the cabin, the air stream passes through the desiccant bed that adsorbed moisture from the previous half cycle. The wet desiccant bed desorbs this moisture to the air stream and returns it to the cabin atmosphere. This is called a water-save system, in contrast to the 2-bed Skylab system, which vented adsorbed water to space.

The alternate CO_2 sorbent bed desorbs by heating with integral electrical heaters and application of space vacuum or, for ground testing, a simulated space vacuum. The heat supplied by the electrical heaters serve two purposes; it breaks the bond the CO_2 has with the sorbent material, and in the subsequent half-cycle heats the passing air-stream to dry out the desorbing desiccant bed. For the first 15 minutes of each half-cycle, the air-save pump operates to remove residual air from the sorbent beds and return it to the cabin.

ON-ORBIT ANOMOLIES

Three CDRA components failed during operation on orbit. A Test Teardown and Evaluation (TT&E) was conducted for each component following return of the hardware to Earth. In every case, the root cause of the failure was found to be free sorbent particles. The failed components were the air-save pump, check valve, and selector valves[2, 3, 4, 5].

A TT&E was also performed on the sorbent and desiccant beds. It was found that the technique used to retain the sorbent particles greater than 50 microns in size inside the sorbent beds had failed and was allowing an indeterminate amount of sorbent material with sizes up to the diameter of a full pellet into the assembly.[3]

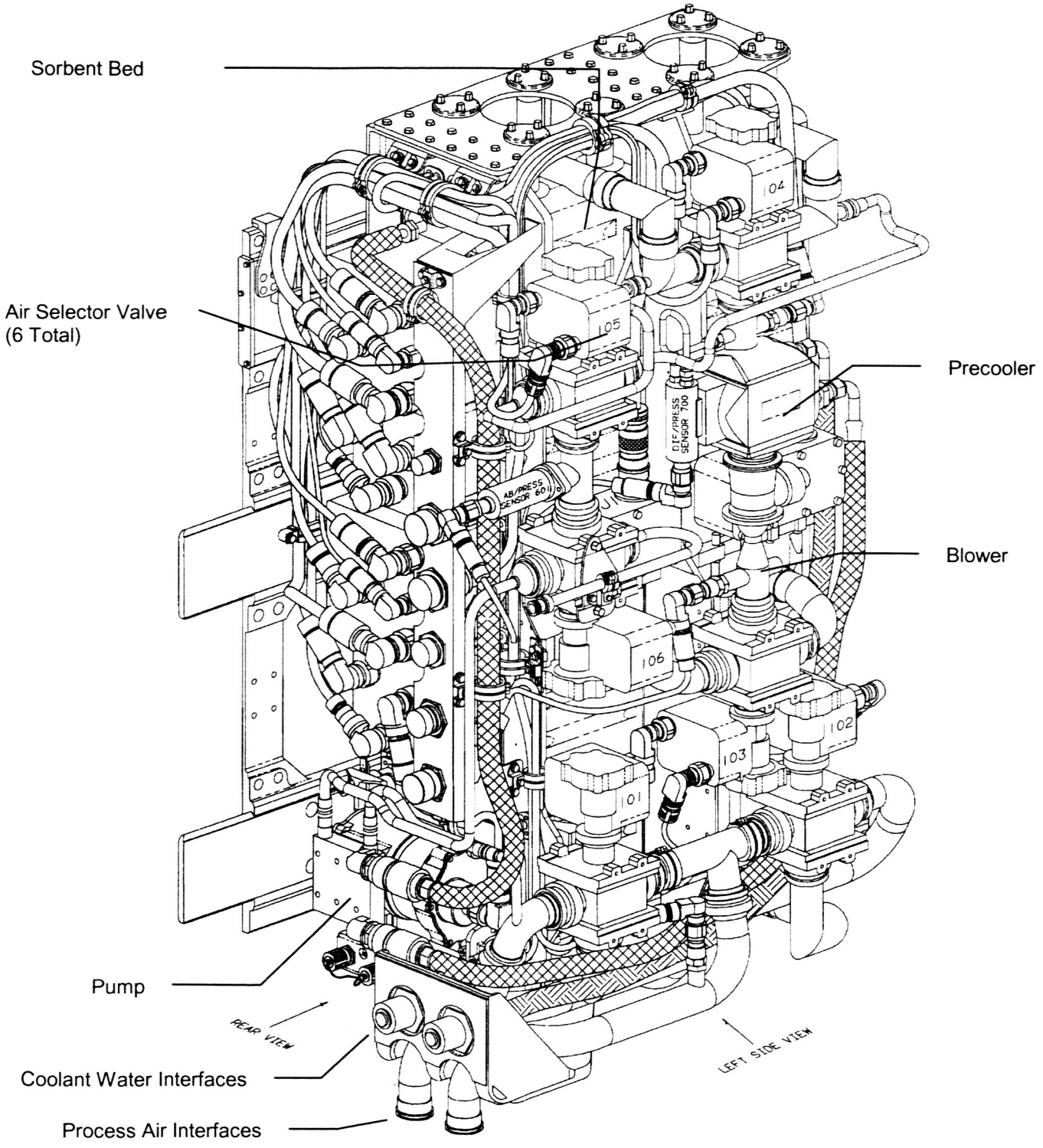

Figure 1. CDRA Flight Hardware [1]

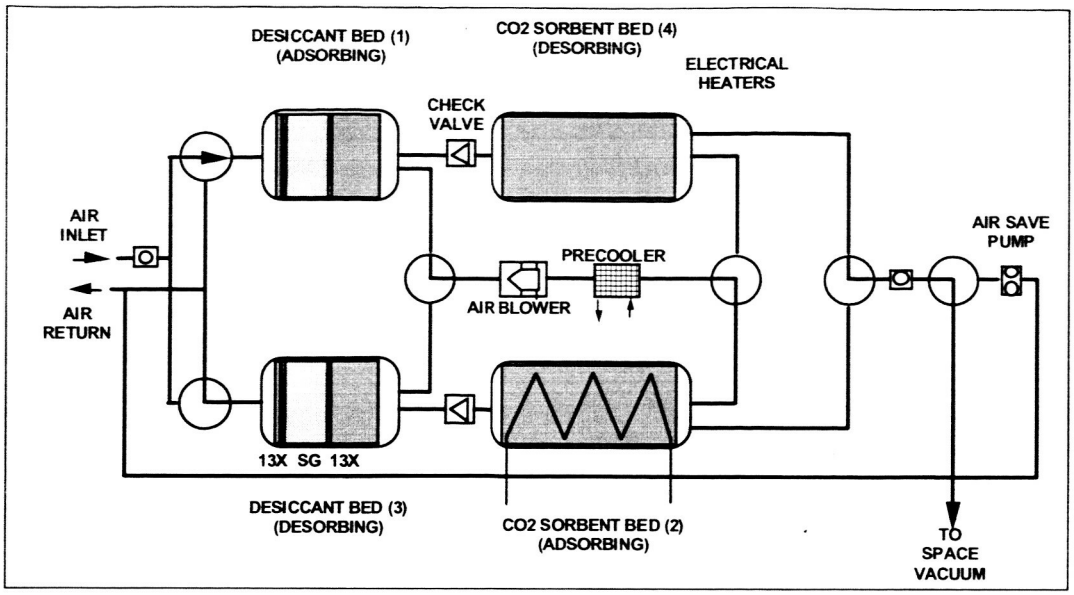

Figure 2. CDRA Schematic

OVERALL CDRA BED CONTAINMENT REDESIGN APPROACH

Recovery from the component failures and correction of the failure root cause (sorbent bed containment design failure) consists of three broad areas:

1. Repair and refurbishment of failed components, to return them to flight status
2. Development and implementation of a in-line filter to protect downstream components from sorbent particles. This is a temporary measure provided only for the on-orbit (Lab) CDRA until step 3 below can be completed
3. Development and implementation of a new sorbent retainment design

The purpose of this paper is to report on the development portion of step 2 above. MSFC supported the development of the in-line filter by providing design data to Honeywell International, the manufacturer of the CDRA.

IN-LINE FILTER DESIGN

PURPOSE: The purpose of the inline filter is to remove sorbent dust down to the lowest practical level while minimizing increased differential pressure. Differential pressure increase must be considered for both a clean and loaded filter. As a design goal, a maximum total system pressure increase of 2.24 inches of water was chosen based on limiting blower speed increase of 2500 RPM (2% of total speed).[6]

CANDIDATE CDRA IN-LINE FILTER LOCATIONS: The primary hardware protected by the in-line filters is the selector valves. These have experienced repeated failures during on-orbit operation, and can be protected by placement of in-line filters in locations with relatively easy crew access. The air-save pump, already protected from large sorbent particles by in-line filters with 250 micron absolute filtration rating, will receive additional protection from filters placed at the air selector valve inlets. Unfortunately, the check valve resides between the desiccant and sorbent beds, a location not accessible without extensive disassembly.

The tubing connecting the air selector valves to the sorbent beds provides a candidate location for the in-line filters. These locations are shaded in Figure 3. It is evident that the straight tube length is limited in all these locations, making use of a long element difficult.

Another option is the ducting integral to the beds, as shown in Figure 4. Although the sorbent bed (top) duct offers no advantages, the desiccant bed integral duct is obviously provides the longest straight length, as well as a large screen area open to flow inside the bed.

Based on these observations, the duct integral to the desiccant bed was chosen to house the filter used to isolate the desiccant bed. The sorbent bed filter is to be housed in the duct connecting the sorbent bed with valve 103, and would be considerably shorter due to limited straight length

CREW ACCESS: Difficulty of crew access can be visualized with the help of Figure 5. The CDRA is mounted on slides for maintenance and removal; however, the CDRA cannot be slid out without first tilting the rack forward and disconnecting fluid interfaces. Since the valves face the major constituent analyzer (MCA), a second option is to remove the MCA first and

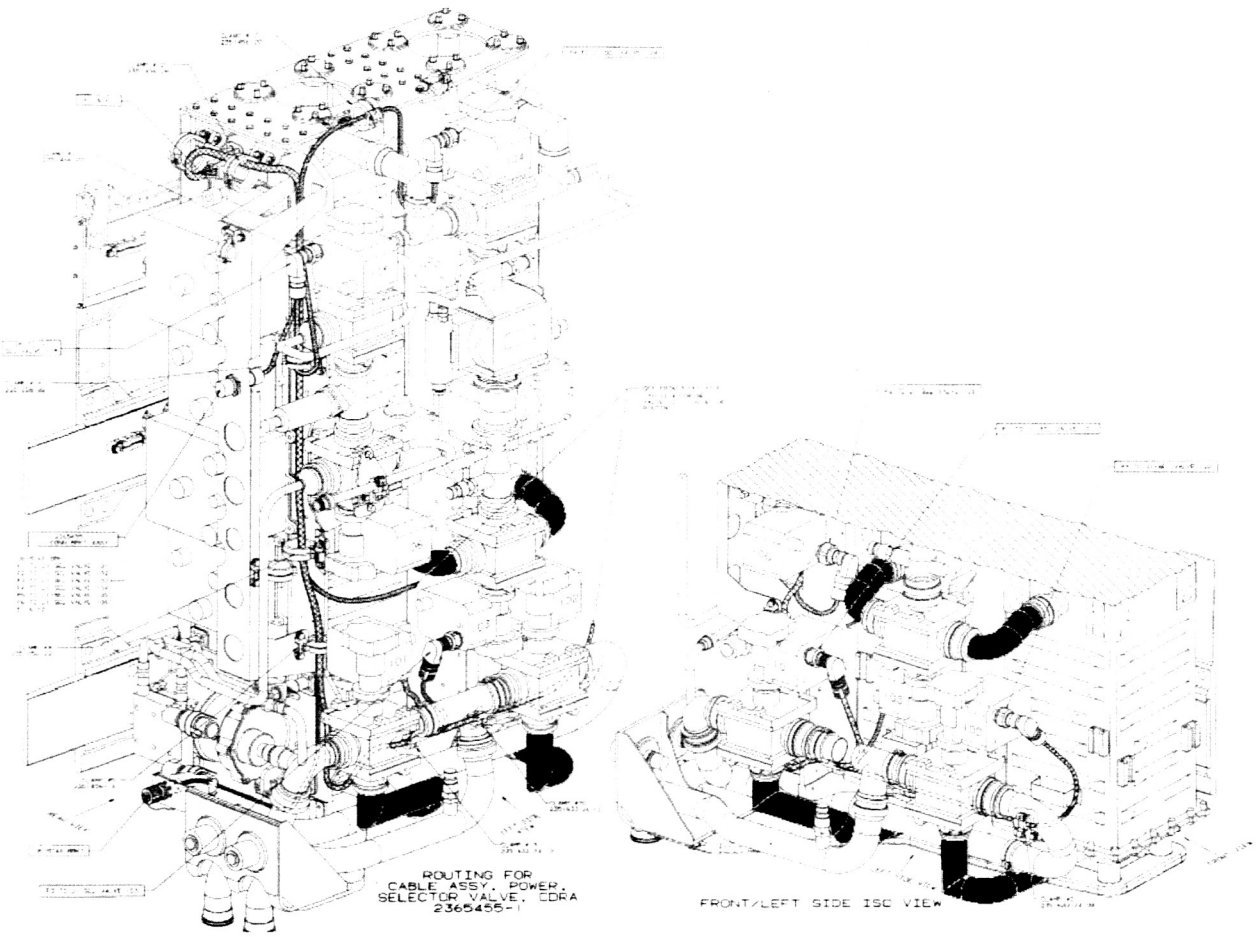

Figure 3. Candidate CDRA In-Line Filter Locations (Isometric View)

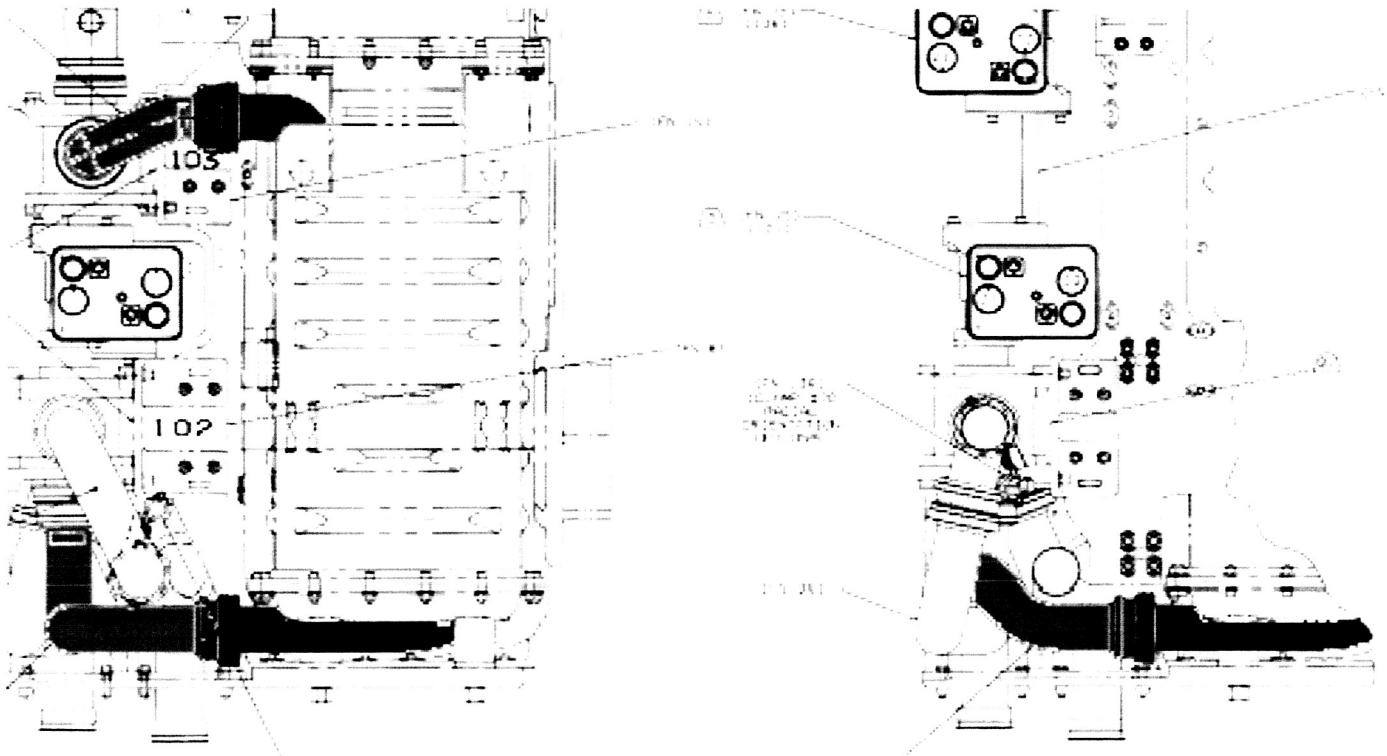

Figure 4. Candidate CDRA In-Line Locations (Side View)

then remove the CDRA ducts for access to install or clean the in-line filters. However, this option is only viable

for the valve 103 in-line filters; the desiccant bed filter location is too low in the rack and will require partial removal of the CDRA.

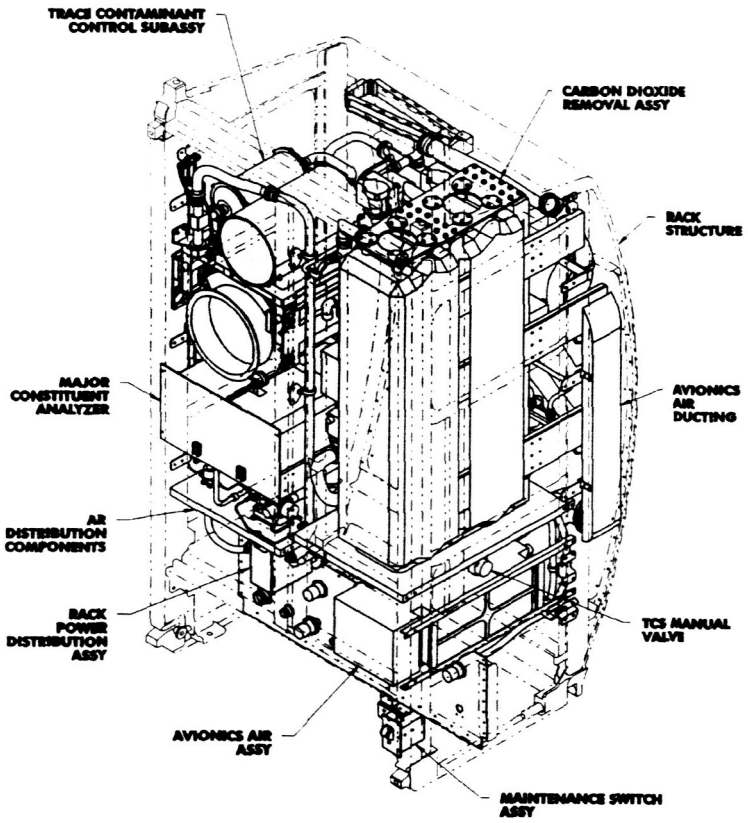

Figure 5. Atmosphere Revitalization Rack[1]

SURVEY OF FILTER MEDIA: To ascertain the applicability of various filter media types, permeability data was collected and compared. This data is shown in Figure 6.

As shown by the defining equations for permeability (Equations 1), the relationship between pressure differential and flowrate is linear; this only applies for laminar flow, whereas the CDRA process air flow in 1.5 inch ducts is fully turbulent. However, the permeability provides for a method of screening media types and selecting a range of micron ratings that are appropriate to the specific application. As shown in Figure 6, permeability (and differential pressure) has an inverse relationship with micron rating.

Figure 7 provides pressure drop estimates for four basic filter geometries using permeability factors. For clarity, only two media types are shown; woven wire mesh (Rigimesh) and sintered metal powder on sintered woven wire mesh (PMM). Micron ratings are shown for each data point. It is evident that the pressure drop will be unacceptable for even the largest surface area geometry (the truncated cone) for media with micron ratings less the 25, eliminating all media types except woven wire mesh.

$$\Delta p = \frac{\zeta Q \eta}{\eta_{air} A} \text{ where}$$

$$\zeta \Rightarrow \text{permeability} \left(\frac{\text{psid} - \text{ft}^2}{\text{scfm}} \right)$$

$$\eta_{air} \Rightarrow \text{viscosity of air } (0.018 \text{ centipoise})$$

$$Q \Rightarrow \text{gaseous flow rate} \left(\frac{\text{actual ft}^3}{\text{min}} \right)$$

$$A \Rightarrow \text{total filtration area } (\text{ft}^2)$$

Equations 1. Permeability Equations

$$\zeta_{wir} \equiv \frac{\Delta p}{\rho w_1^{\,2}/2} = 1.3(1-\bar{f}) + (\frac{1}{\bar{f}} - 1)^2 \text{ where}$$

$$\bar{f} = \frac{F_o}{F_1} \text{ (fraction screen open area)}$$

$$50 < \text{Re} < 10^3 : \zeta_{\text{Re}} = \frac{\Delta p}{\rho w_1^{\,2}/2} = k'_{\text{Re}} \zeta_{wir}$$

$$\text{Re} < 50 : \ \zeta_{\text{Re}} \approx \frac{22}{\text{Re}} + \zeta_{wir}$$

Equations 2. Idelchik Correlations for Plain Square Mesh, Circular Metal Wire

$$hf_i = 1.00 \text{ perpendicular surfaces}$$

$$hf_i = 0.55 \text{ non-perpendicular surfaces}$$

$$w_1 = \frac{\dot{V}}{\sum_i hf_i A_i}$$

(linear velocity adjusted for housing factor)

Equation 3. Initial Adjustment for Non-Perpendicular Flow

PRE-TEST ANALYSIS OF WOVEN WIRE MESH: To determine the appropriate micron rating for plain square weave (PSW) mesh media, one can use a series of correlations published by Idelchik[7] shown above. This correlation accounts for flow regime by incorporating the Reynolds number. In addition, an estimate was made in Equation 3 based on Idelchik for the effect of non-perpendicular flow. This turned out to be highly underestimated, however, based on later test data.

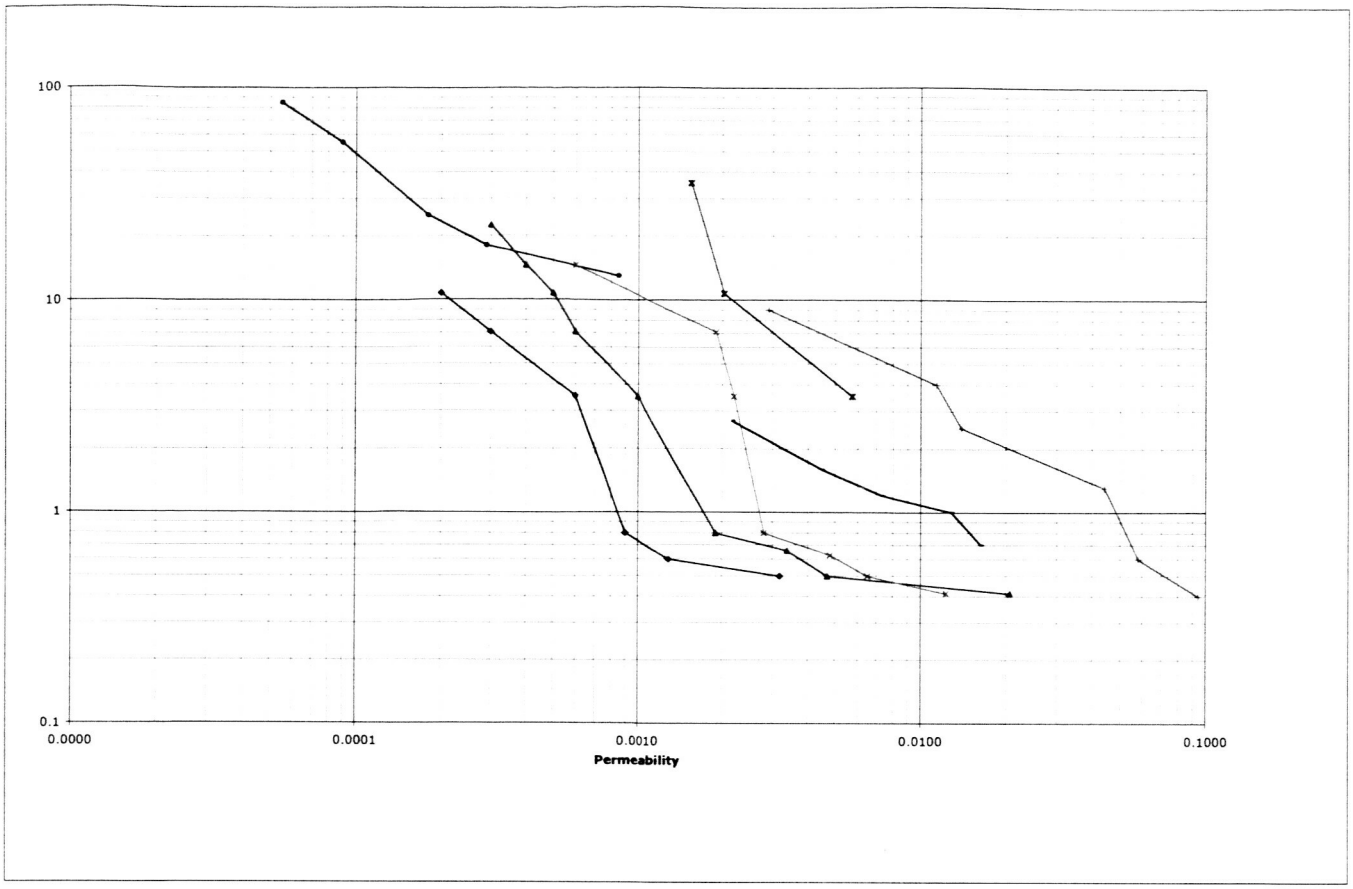

Figure 6. Permeability vs. Absolute Micron Rating in Gas Service

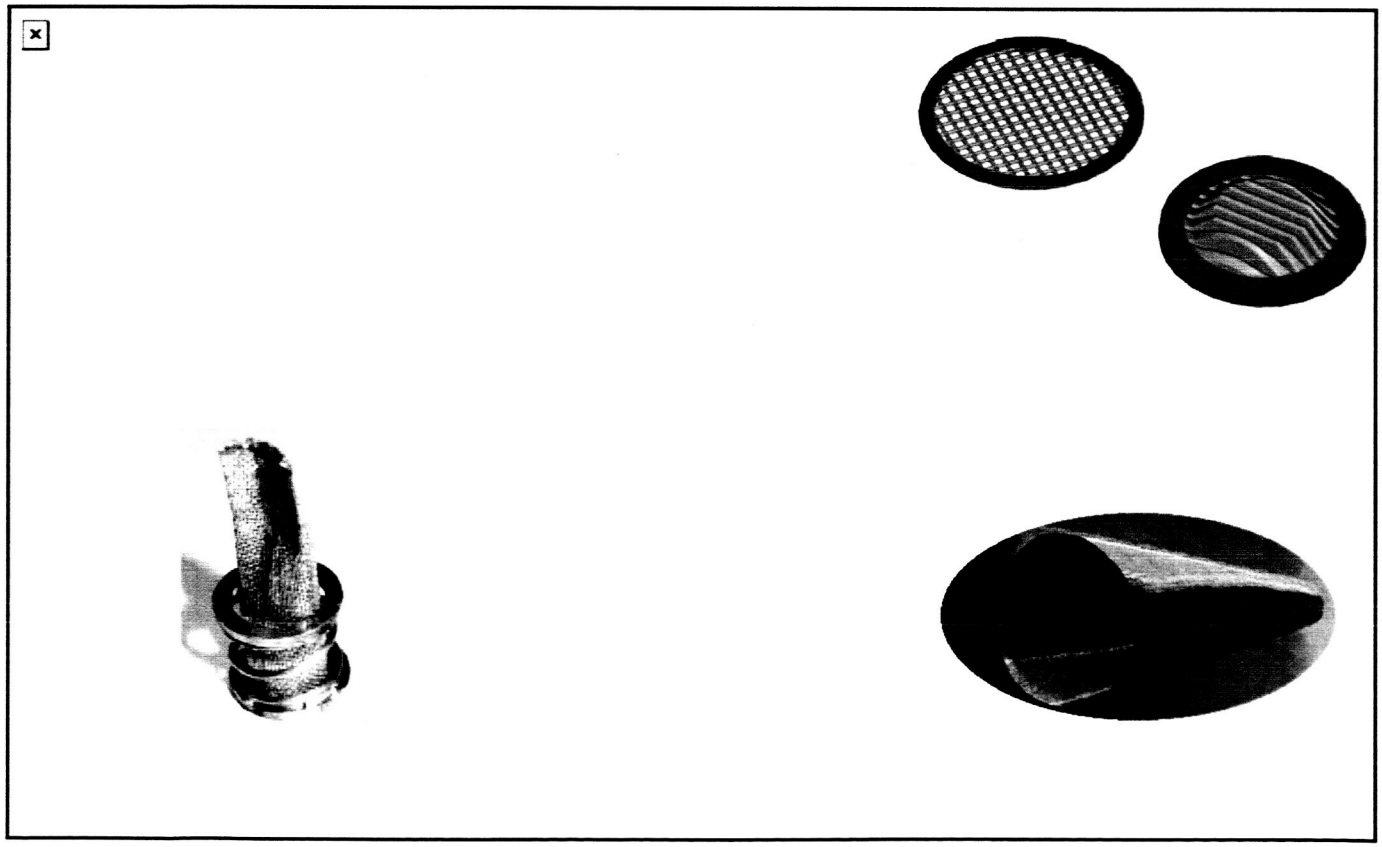

Figure 7. In-Line Filter Pressure Drop for Various Geometries Based on Permeability Factors

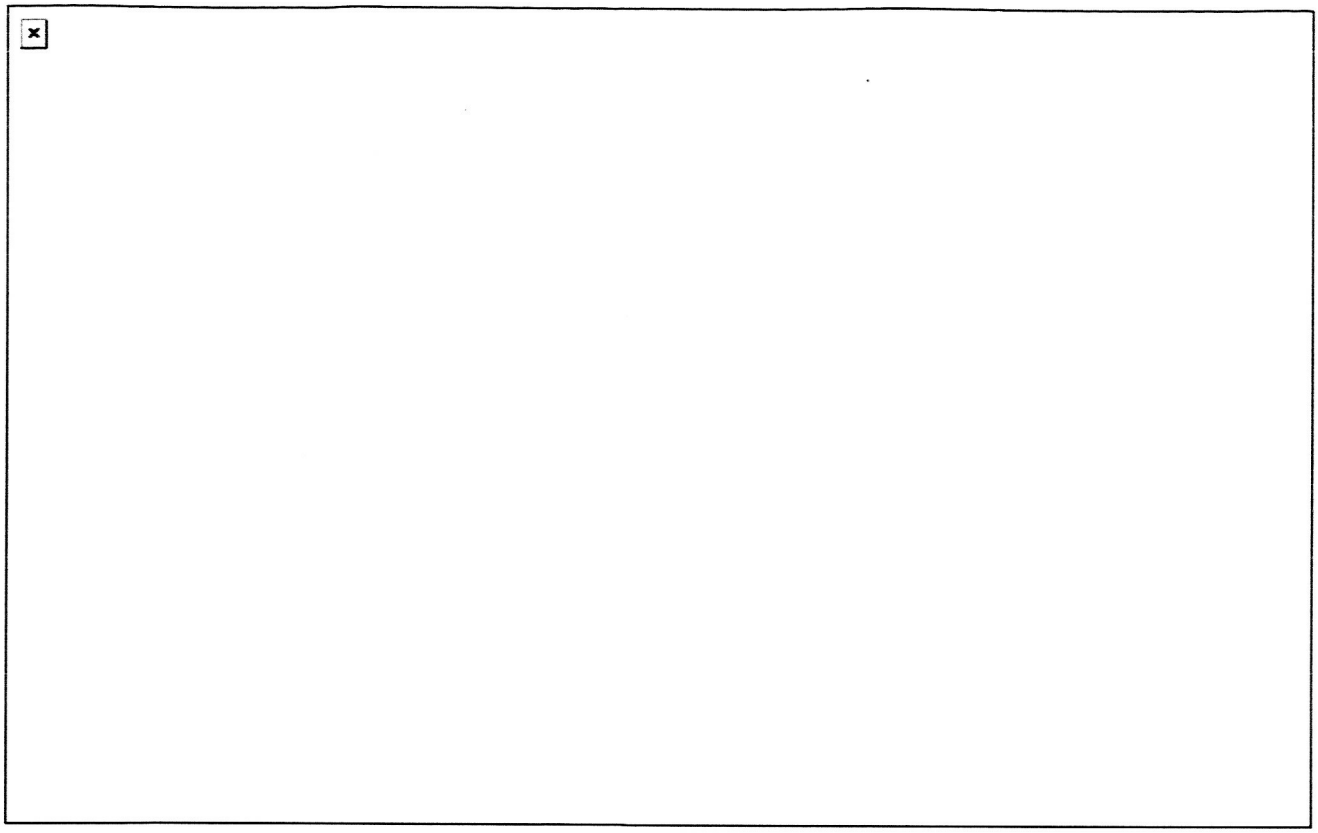

Figure 8. Pressure Drop and Surface Area for 53 Micron Screen

The Idelchik equations were used in conjunction with the CDRA sorbent bed screen micron rating of 50 to select a market grade, or common configuration, of plain square weave with a micron rating of 53 microns. Figure 7 was repeated with the Idelchik correlations for this mesh in Figure 8, along with surface areas for the various geometries. Surface area provides a measure of tolerance to loading with respect to pressure differential. This chart indicated that the pleated disc would sharply reduce pressure drop, but provide only a moderate increase in tolerance to dust loading. The pinched cone and truncated cone geometries provide both a large decrease in pressure differential and increase in loading tolerance.

PRESSURE DIFFERENTIAL TESTING

A pressure differential test rig was built at MSFC specifically for support of the in-line filter design. Shown in Figure 9, this test rig provides comparative data for a range of screen micron ratings and for various filter element configurations. The rig matches actual tube diameter and flow rate. Pressure measurement ranges are 0 to 2, 0 to 5,0 to 10, and –25 to 25 inches of H2O absolute.

Use of the pressure differential rig with dust injection provided comparative data for various filter element configurations as they load with zeolite dust.

CLEAN ELEMENT DIFFERENTIAL PRESSURE TESTS: Test was conducted with a variety of media types, including plain and pleated discs, plain cones, and cone-tipped cylinders. The latter two elements were constructed at MSFC of the 53 micron screen material. Two-ply materials were tested, with two different meshes sintered together for progressive filtering and protection of the fine filter. In total, 28 filter media types were evaluated.

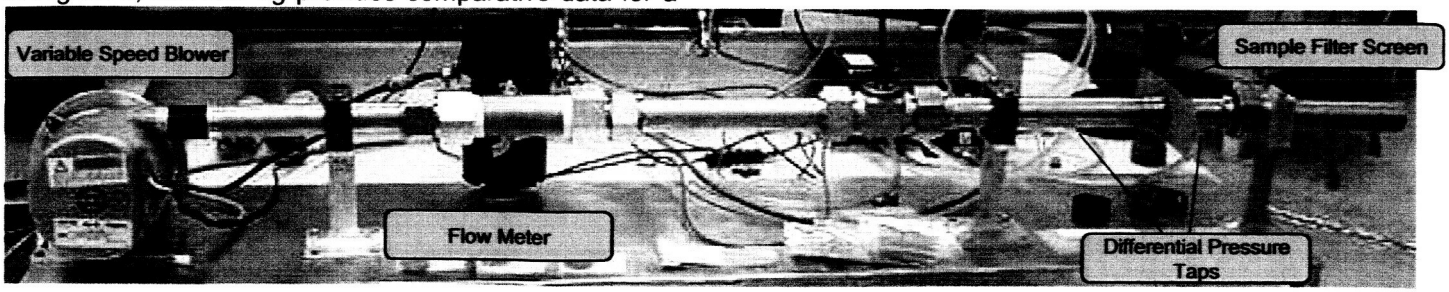

Figure 9. Filter Media Pressure Differential Test Rig

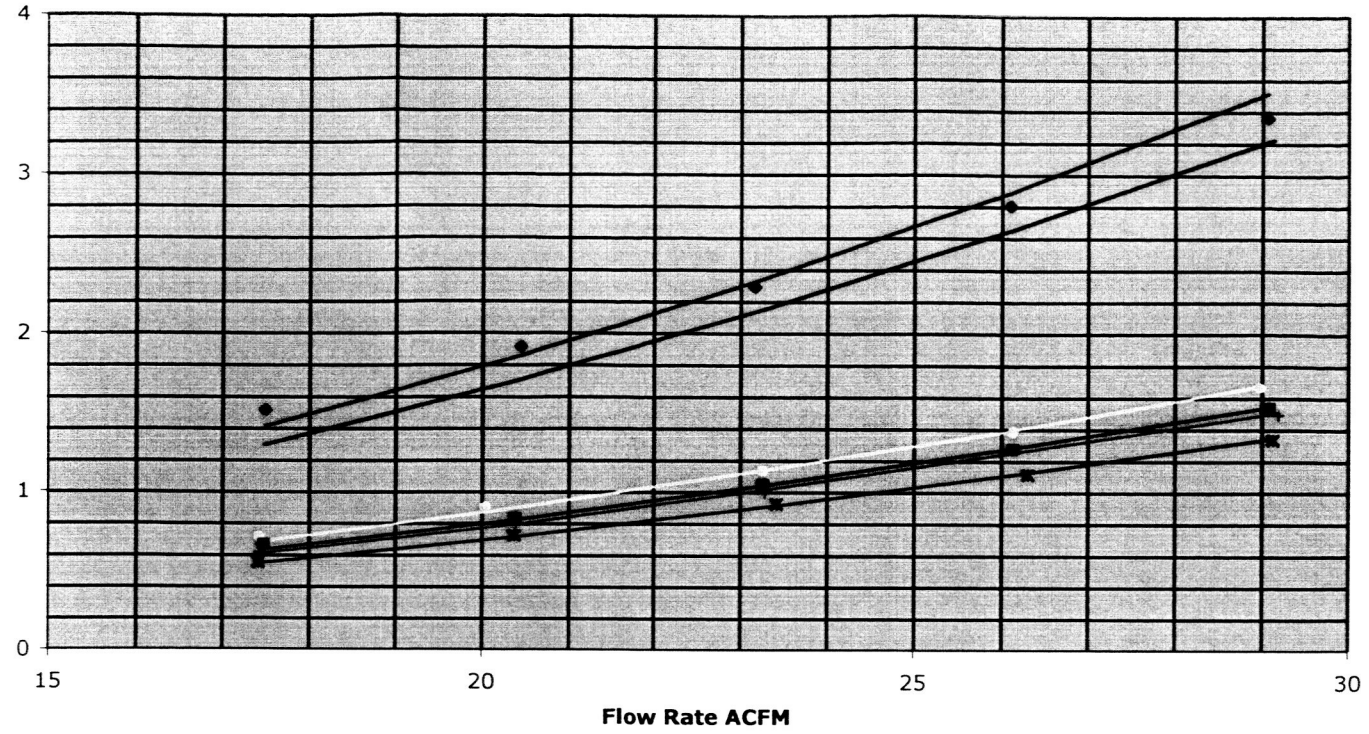

Figure 10. Flow Resistance of 270 Twill Mesh (53 micron) in a 90° Tube with No Dust Loading

Single-Ply Test Data and Correlation: Sample test results are shown in Figure 10. Plotted are the test data, as discrete points, and simulated data, as lines, based on the Idelchik correlation

The results in Figure 10 show a reasonable match between test data and the Idelchik correlation. As mentioned previously, a percent effectively of 55% for non-perpendicular surfaces was non-conservative. Table 1 below provides the effective area used to provide a best fit to test data for each of the geometries. For the pleated disc, data from another mesh type was used to derive the effective area. The effective area is used later for prediction of pressure drop in the two-ply mesh configurations.

Element Type	Effective Area
Disc	100%
Pleated Disc	19.5%
Cone-Tipped Cylinder in Upstream Orientation	21.4%
Cone-Tipped Cylinder in Downstream Orientation	22.3%
Cone in Downstream Orientation	33%
Cone in Upstream Orientation	24.8%

Table 1. Effective Areas for Various Geometries

Comparing the element geometries at the target flowrate using the verified correlations results in Figure 11. Comparing these results with Figure 8 shows that the pleated disc in actuality offers only a moderate decrease in pressure drop over the disc. The results indicate that the cone achieves the lowest pressure drop, but that the cone-tipped cylinder provides higher surface area. This would indicate a greater tolerance to dust loading for the cone-tipped cylinder. In order to examine these conclusions, testing was next conducted with sorbent dust particles.

Dust Loading Tests: To provide comparative data on the pressure differential for the cone-tipped cylinder and plain cone, a quantity of 5A molecular sieve sorbent was ground in a mortar and pestle to provide a range of particle sizes. The sorbent was allowed to equilibrate at room temperature and humidity, weighted, then completely desorbed. The change in weight was nearly 25%. This data was used to calculate the dry weight of the dust injected into the filter elements.

For the initial round of tests, approximately 1 gram of dust was injected into the cone-tipped cylinder in both downstream and upstream configurations. As shown in Figure 12 below, this amount of dust increased the pressure drop for the downstream configuration by nearly 1.5 inH2O with fan speed unchanged.

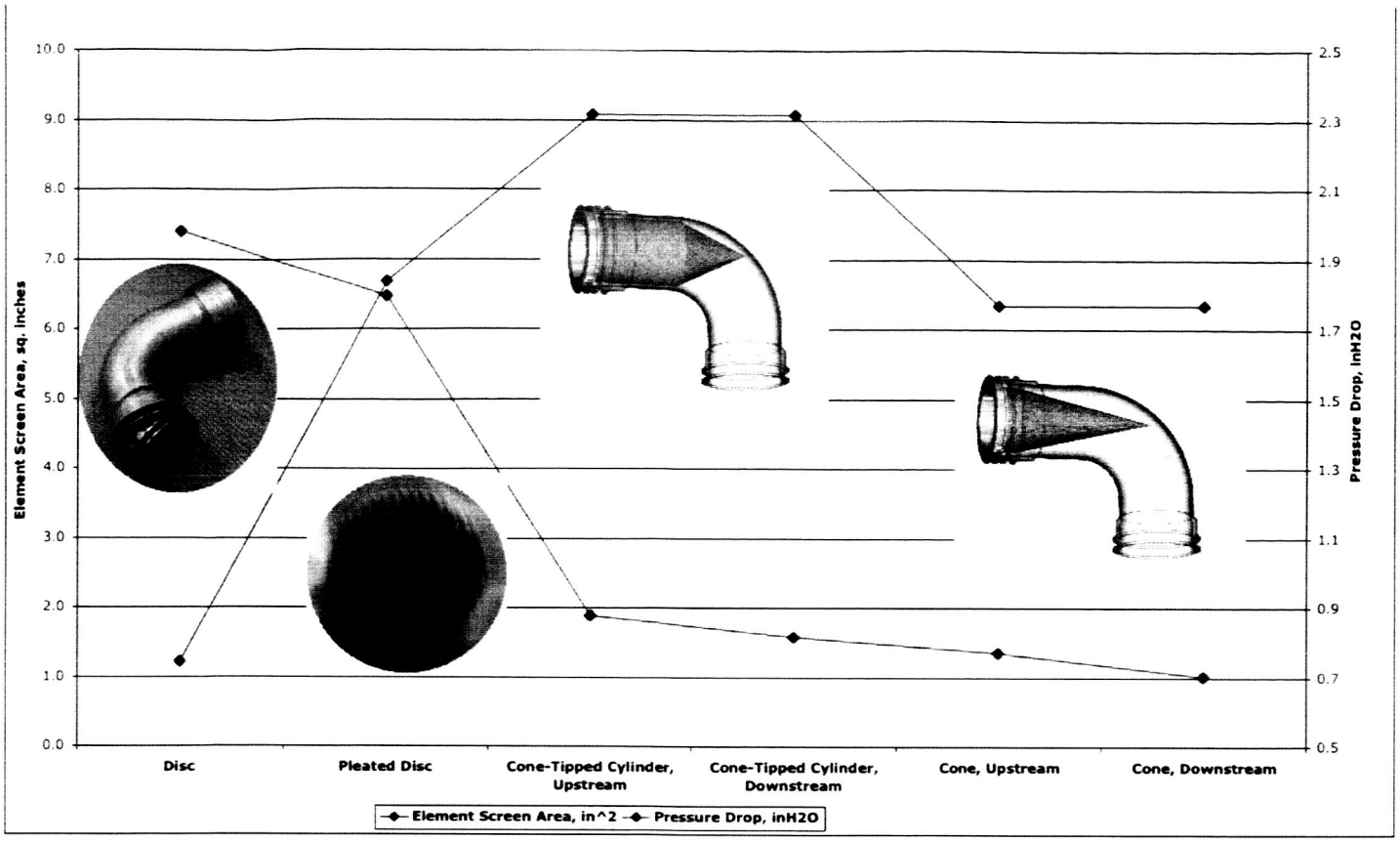

Figure 11. Geometry Comparison for 270 Twill Mesh at 20 AFCM; Idelchik Equation Correlated to Test Data

Figure 12. Dust Loading vs. Pressure Drop in 90° Tube at 20 SCFM

Once the fan speed was increased to restore the flow rate to 20 scfm, the total pressure increase was nearly 3 in Hg. It is speculated that the dramatic increase was due to the dust accumulating in the primary flow area, the tip of the cone, for this configuration.

Pressure increases for the downstream orientation of the cone-tipped cylinder and both orientations of the cone are much less dramatic. Off all the configurations, the pressure drop for the upstream facing cone is least sensitive to dust loading.

SELECTION OF FILTER ELEMENT AND ORIENTATION: The combined results of the clean and loaded pressure drop testing indicated that the upstream facing cone is the superior candidate for further development.

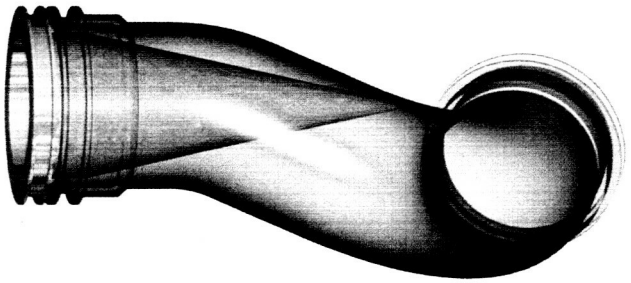

Figure 13. Cone Filter Element in Downstream Orientation in Flight Duct

DESICCANT BED FILTER ELEMENT: Not discussed thus far is the second location for isolation of sorbent material, that is, the desiccant bed inlet duct. Due to the longer allowable length of this element, a low pressure differential could be expected. This was confirmed by testing at 20 scfm to be 0.21 inH2O for the 53 micron screen. No further optimization was considered necessary.

ADDITION OF A SUPPORT MESH: The wire used for the 270 twill, 53 micron mesh is rather fine, at 0.0016 inch diameter. We noted during testing that this mesh was easily creased by handling. As such, a support mesh was considered. Initially, a PSW mesh with 62 0.0045" diameter wires per inch was sintered to the 270 twill material by Martin Kurz & Company. Testing of this mesh, however, indicated a higher than acceptable overall pressure drop.

The second support mesh considered was a PSW with 42 0.0055" diameter wires per inch. Martin Kurz & Company also sintered this to the 270 twill mesh, with acceptable pressure differential. This 2-ply mesh was used to fabricate the flight filters, which are currently on orbit awaiting installation in the Lab CDRA.

CONCLUSIONS

A design exercise has been conducted to optimize the geometry and filter media to be used for isolation of sorbent dust within the packed beds of the on-orbit CDRA until the failed sorbent containment can be redesigned and replaced. A combination of test and analysis was used to determine the optimal mesh (270 twill with a 53 micron rating) and configuration (a simple cone) and orientation (upstream to the flow).

Due to the small wire diameter of the chosen mesh, it was sintered to a support mesh (42 PSW mesh). The final cone, fabricated by Honeywell Space Systems, was flown on flight 14p to the International Space Station.

CONTACT

James C. Knox
Mail Stop FD21
Marshall Space Flight Center
Huntsville, AL 35812
Telephone: (256) 544-4887
E-mail: James.C.Knox@msfc.nasa.gov

REFERENCES

1. Environmental Control and Life Support (ECLS) Architecture Description Document, Volume 2, Book 2, Revision C, D684-10508-02-02, Boeing Defense and Space Group, Houston, 1999

[2] CDRA Air-Save Pump TT&E Report
[3] CDRA Bed and Valve TT&E Report(TT&E Report Bed ORU.pdf)
[4] CDRA Air Selector Valve TT&E Report(TT&E Report Selector - 1107F.pdf)
[5] Richard Reysa, Matt Davis, Dina El Sherif, "International Space Station (ISS) Carbon Dioxide Removal Assembly (CDRA) Anomaly Resolution, SAE paper 2003-01-2486
[6] Email from M. Russell, 5-13-03 (Calcs for CDRA Blower - FFD5.eml)
[7] Idekchik, I. E., "Handbook of Hydraulic Resistance, 3rd Edition, CRC Press, 1993